Evaluation of Antimicrobial, Cytotoxicity and Catalytic Activities of CuO-NPs Synthesized by Tanacetum Parthenium Extract

Mojtaba Ranjbar (ranjbarf@ausmt.ac.ir)
Amol University of Special Modern Technologies
Mahsa Dastani
Amol University of Special Modern Technologies
Fatemeh Khakdan
Women's University of Semnan,

Research Article

Keywords: Tanacetum parthenium, Catalytic dye degradation, Antimicrobial activity, Pharmaceutical

DOI: https://doi.org/10.21203/rs.3.rs-154772/v1

Abstract

Development of efficient methods for treating microbial infections, cancer, and toxic organic dyes is *a serious* challenge in medical sciences. The purpose of this study is to synthesize CuO-NPs using *T. parthenium extract* and to evaluate its anticancer, antimicrobial, and catalytic activity. CuO-NPs were characterized by UV-Vis, XRD, FTIR, FESEM, and EDX. UV-Vis spectra exhibited surface plasmonic resonance at 298 nm of synthesized CuO-NPs. The synthesized CuO-NPs were pure, predominantly spherical with mean size of 16 nm. FTIR confirmed that CuO-NPs were reducted and stabilized with the biomolecules present in the *T. parthenium extract*. CuO-NPs indicated excellent degradation activity for the industrial dyes, i.e., MO (96.6% removal in 400s), Rh B (98.3% removal in 400s), MB (98.7% removal in 400s) and CR (99.6% removal in 180s). CuO-NPs showed excellent inhibition against selected microorganisms, especially *E.coli* and *C. albicans*. CuO-NPs *have also* shown good anticancer activity against A549, Hela, and MCF7 cancer cell lines (IC50 = 65.0, 57.4, and 71.8 µg/mL, respectively) while negligible cytotoxic effects were observed on L929 (IC50 = 226.1 µg/mL). The results proposed that synthesized CuO-NPs can be considered as a suitable candidate for biomedical, pharmaceutical, and environmental applications.

Introduction

Nanoparticles (NPs) have broad applications in pharmaceutics, biomedicine, cosmetics, space technology, electronics, catalytic, and environment[1]. NPs possess several exceptional and useful properties as compared with bulk materials with similar chemical composition. High yield strength, quantum size, high surface-to-volume ratio, rigidity, plasticity, hardness, and macro quantum tunneling effect are the most important properties of NPs[2]. Currently, CuO-NPs have attracted considerable interest due to their low cost and acceptable stability[3, 4]. CuO-NPs are used as diagnostic tools and therapeutic agents against microbial infections, cancer and it is also applied as a clearing agent against synthetic organic dyes from water[5–8]. Physical and chemical methods can produce pure nanoparticles, but they are not efficient methods. Biosynthesis of NPs using green chemistry based methods is cost-effective, non-toxic, and eco-friendliness[9]. Several methods have been applied to produce green synthesized nanoparticles using bacteria[10], plants[11], yeast[12], fungus[13], and viruses[14]. Plant based nanoparticle synthesis has several advantages over other methods, including cost-effectiveness, fast production, simplicity, non-toxicity and biocompatibility[11]. The biosynthesis of CuO-NPs has been successfully attained using the extract of *E. prostrate*[15], *P. asiatica*[16] and *Rhuscoriaria L.*[17]. However, the potential of plants aqueous extracts as natural materials for synthesizing metal nanoparticles is yet to be fully explored. The plant *Tanacetum parthenium* grows in moderate regions of Asia, Europe, North and South America. It belongs to the family of Asteraceae and which is known as a perennial plant[18]. In traditional medicine, this herb is used to treat thrombotic thrombocytopenic purpura, spasmodic pains, inflammation and microbial infections. These medicinal features have been related to the presence of several bioactive compounds such as sesquiterpenes, coumarins, flavonoids, flavones and tannin[18, 19]. In the present study, an environmentally compatible method for the preparation of CuO-NPs using *T. parthenium* extract

as reducing and stabilizing agents has been described. The catalytic activity and clearing effects of synthesized CuO-NPs were also examined on organic dyes. The antimicrobial activity of CuO-NPs against *E. coli, S. typhimurium, P. oryzae*, *F. thapsinum*, *C. albicans*, and *C. neoformans* was tested using disc diffusion method. Using MTT assay, the inhibitory effect of CuO-NPs was also evaluated against Hela, MCF7, A549, L929 cell lines.

Results And Discussion

Chemical characterization of CuO-NPs

The UV–Vis absorption spectrum of *T. parthenium* extract (Fig. 1) demonstrates that peaks at 290 and 320 nm are allocated to the π→π* or n→π* transitions, which can be attributed to the presence of polyphenols compound. The change of solution color corroborated the synthesis of CuO-NPs using *T. parthenium* extract from pale yellow to caramel brown Fig. 1. Further verification was performed using UV–Vis spectroscopic analysis, and the maximum peak was viewed at 298 nm, emphasizing CuO production from copper sulfate (Fig. 1). According to the results, the main characteristics of resonance band of the sulfate Plasmon at 298 nm happened for copper nanoparticles. The result here is compatible with previous studies on the biosynthesis of CuO-NPs using *R. tuberosa* and *P. guajava* leaves extract[6, 7].

FTIR spectral was performed to identify the biomolecules from *T. parthenium* extract that might be responsible for the reduction, stability, and synthesis of CuO-NPs. The representative FTIR spectra of the aqueous extract and the biosynthesized CuO-NPs are showed in Fig. 2. The absorption bands at 3430.44 and 3429.25 cm^{-1} are due to O-H stretching of phenols and alcohols[20, 21]. The bands at 2926.0 and 2924.14 cm^{-1} originated from C-H stretching vibrations of methyl groups of the lipids[3]. The absorption bands at 1625.5 and 1624.5cm^{-1} have corresponded to the amide I in proteins and C = C in aromatic compounds[20]. The bands at 1408.1 and 1386.3 cm^{-1} were probably related to COO- in the amino acid residue of protein and CH_3 stretch of fatty acids[3, 22]. The bands at 1256.5 and 1260.1 cm^{-1} could be due to the C-O group stretching vibration of carbohydrates and amide III for protein[23]. The bands at 1069.4 and 1057.6 cm^{-1} might be related to the C-O stretching band of oligosaccharide residue[3]. The bands at 616.9 and 611.1 cm^{-1} are probably attributable to the alkyl halide[24]. The first and second numbers belong to the aqueous extract and CuO-NPs, respectively. Comparing the result obtained from aqueous extract and CuO-NPs showed that the peaks observed in the spectrum of the aqueous extract are also present in the spectra of synthesized CuO-NPs with lower severities and a slight variation. After synthesizing CuO-NPs, the absorption peaks at 3,430, 2926, 1625, 1408, and 1,069 cm^{-1} observed in aqueous extract get thinner and changed to low-frequency regions. FTIR analysis results were in agreement with the FTIR spectrum pattern of the *B. tomentosa* leaves extract, which proposed phytochemical compounds such as proteins and polyphenol contributed to the synthesis of CuO-NPs[25].

Crystalline feature confirmation of CuO-NPs was characterized by XRD analysis (Fig. 3). XRD patterns of CuO-NPs synthesized by green method demonstrate notable peaks at 2θ of 32.65˚, 38.7˚, 48.8˚, 53.4˚,

58.35˚, 61.65˚, 66.35˚ and 75.45˚ which were allocated to the (110), (111), (202), (020), (202), (113), (311) and (004) planes. The observed diffraction data were comparable with JCPDS No. 45-0937[20]. The present results are in good agreement with the previous report on the synthesis of CuO-NPs using *A. hispidum* aqueous extract[20].

The morphology and particle size of the synthesized CuO-NPs were evaluated by FESEM analysis. The FESEM results showed the globular figure with the range size nearly from 13 to 25 nm and average size around 16 nm, which corroborating the formation of CuO-NPs by extract of *T. parthenium* (Fig. 4a). Similar morphology was achieved for CuO-NPs when it was synthesized by *R. Crispus* extract and *P. hexapetalum* leaf extract[27, 28]. EDX was applied to identify the elements of the synthesized CuO-NPs by *T. parthenium* extract (Fig. 4b). The signals corresponding to carbon (14.38%), oxygen (30.37%), copper (49.38%), phosphorus (3.88%), and sulfur (1.99%) identified in CuO-NPs EDX spectrum and the Cu signal intensity authenticated the formation of CuO-NPs. Carbon, phosphorus and sulfur signals are emanated from the biomolecules of *T. parthenium* extract detected on the nanoparticles plane. EDX result was in agreement with previously reported results on synthesized CuO-NPs[3, 25, 29].

Catalytic activity evaluation for reduction of MO, RhB, MB and CR dyes

Industrial dyes are released into the water and aqueous environments; hence they are considered as a major threat to the ecosystem, aquatic life, and creature's health. Methylene Orange (MO), Rhodamine B (RhB), Methylene Blue (MB), and Cango red (CR) lead to several health hazards such as breathing, vomiting, nausea, and diarrhea[7, 30]. As a result, there is a great interest developing modern methodologies that can remove and degrade industrial dyes. These dyes are stable molecules, and their reduction by $NaBH_4$ in the absence of any suitable catalyst occurs at a prolonged rate. This prolonged rate may be due to the large redox potential difference between an electron donor ($NaBH_4$) and an electron acceptor (MO, RhB, MB, and CR)[31, 32]. CuO-NPs serve as nanocatalyst, capable of accepting electrons from an electron donor and transfer them to the electron acceptors (industrial dyes). The catalytic reductions of MO, Rh B, MB, and CR with an extra amount of $NaBH_4$ were selected as model reactions to appraise the catalytic activity of CuO-NPs. As the results indicated, in the absence of CuO-NPs, the reduction reaction did not proceed. On the other hand, in the presence of CuO-NPs, catalytic reduction of the dyes happened. This reduction effect is responsible for the degradation observed in the industrial dyes. It should be noted that the degradation process is continuously increased along with time. Specific peaks for MO, RhB, MB, and CR disappeared thoroughly after 400, 400,400, and 190s, respectively, and the color became lucid, denoting the reaction's completion. Linear relationship between ln (C_t/C_0) versus reaction time confirms that the reactions pursued first-order kinetics. The apparent rate constants (k_t) were calculated from first-order reaction kinetics using the slope of straight lines. The k_t values of CuO-NPs for the reduction of MO, RhB, MB, and CR were 5.8×10^{-3} s^{-1}, 9×10^{-3} s^{-1}, 1.31×10^{-3} s^{-1} and 2.5×10^{-3} s^{-1}, respectively. The highest k_t value of CuO-NPs was observed for the reduction of RhB (9×10^{-3} s^{-1}). The apparent rate constants and dye degradation time of CuO-NPs catalyzed reactions are identified to be comparable and, in some cases, even better than the reviewed catalysts in the articles for the reduction of MO, RhB, MB

and CR[27, 33, 34]. The maximum degradation percentage of MO, RhB, MB, and CR was 96.6%, 98.3%, 98.7%, and 99.6%. The maximum and minimum degradation were observed in Congo red and Methylene Orange, respectively. Recycling and reusing heterogeneous catalysts are among the main subjects in the practical application of heterogeneous catalysts[35]. CuO-NPs heterogeneous catalyst can be retrieved after the completion of the reaction mixture by centrifugation. The UV-Vis absorption results demonstrated that the stability and turnover of the CuO-NPs catalyst in reducing and degrading MO, RhB, MB, and CR can remain unaltered after four consecutive cycles in catalytic reaction[27].

Antimicrobial Activity Of Synthesized Cuo-nps

Significant antimicrobial activity was observed in all concentrations of CuO-NPs against examined bacteria and fungi strains (Fig. 6 and Table 1). The size of inhibition zone increased with increasing CuO-NPs concentration; at 100 µg/ml concentration of CuO-NPs, the maximum inhibition was obtained for *E. coli* (22 mm) and *S. typhimurium* (21 mm). The maximum zone of inhibition (21mm) was observed in *C. albicans* followed by *C. neoformans* and *F. thapsinum* (20mm), and *F. semitectum* (19mm) with 130 µg/ml CuO-NPs (Fig. 6 and Table 1). CuO-NPs showed potent antimicrobial activity against *E. coli* and *F. semitectum* when compared to the positive control. In comparison with bacteria, fungi had a smaller inhibition zone, probably because of the presence of chitin in their cell wall, which exhibits higher resistance to nanoparticle penetration into the inner layer of the cell wall. Similar results were observed when CuO-NPs synthesized using *Cissus arnotiana* extract[36]. The antimicrobial activity of CuO-NPs could be due to the smaller size and the larger surface-to-volume ratio of CuO-NPs allowing nanoparticles to expansively attach with the cell membrane and damage the genetic material, causing cell death[37]. The cell membrane damage caused by the electrostatic interaction between the phosphate groups in the cell membrane. Moreover, releasing the Cu^{2+} ions disrupts cell membrane integrity leading to membrane leakage[34, 37]. Furthermore, the production of reactive oxygen species (ROS) damages DNA, RNA, lipids, proteins, and the activity of certain periplasmic enzymes, restraining ATPase activities from reducing the ATP level[34].

Table 1
Antimicrobial activity of *T. parthenium* extract derived CuO-NPs

Name of the microorganisms	**Zone of inhibition (diameter in mm) at different concentrations**				
	35µg/ml	70 µg/ml	100 µg/ml	130µg/ml	Cip (5µg/disc)/ Amp-B (100units/disc)
S.typhimurium	11	17	21	NT	33
E.coli	12	17	22	NT	Not ZI
F.thapsinum	11	13	15	20	22
C.albicans	9	12	15	21	23
F.semitectum	10	12	14	19	Not ZI
C.neoformans	11	13	15	20	25
Cip: Ciprofloxacin for bacteria; Amp-B: Amphotercin –B for fungi; NT:Not tested; Not ZI: Not zone inhibition					

Anticancer Activity Evaluation Of Synthesized Cuo-nps

In vitro cytotoxic activity of CuO-NPs indicated high level cytotoxicity effect against all of the cancer cell lines compared to L929 normal cells at various concentrations (25–130 µg/mL) (Fig. 7). Cell death recorded at 130 µg/mL concentration of CuO-NPs was almost 12.1%, 8.8%, and 19.9% for A549, Hela, and MCF7 cell lines, while in the case of L929 cell lines, the cell death was only 73% at the same concentration. Both cancer cell lines and normal cell line demonstrated a reducing percentage of cell viability with augmenting concentration of CuO-NPs (Fig. 7).

It can be concluded that increased number and aggregation of CuO-NPs within the cell lines result in enhanced oxidative stress, causing cell death[28]. IC50 values of CuO-NPs were discovered to be 65.0 µg/mL, 57.4 µg/mL, 71.8 µg/mL and 226.1 µg/mL for A549, Hela, MCF7 and L929 cell lines, respectively. Compared to the normal cell lines, lower IC50 value of CuO-NPs in the cancer cell lines can be related to the high reproduction rate, abnormal metabolism, and high uptake of CuO-NPs in cancer cell lines[38]. High cytotoxic effect of CuO-NPs is probably due to their size, shape, and large surface-to-volume ratio which enable the nanoparticles to readily enter the cells[39]. CuO-NPs not only can interact with mitochondria but also can interrupt the cellular electron transition chain, causing to elevated level of ROS which in turn causes

DNA damage, activates apoptosis and signaling pathway of MAPK, and consequently cancer cell lines death[40]. Several studies reported increased level of- ROS formation in cancer cell lines during treatment

with nanoparticles[41, 42].

Conclusions

We have successfully biosynthesized CuO-NPs through eco-friendly, low cost, and simple method using aqueous extract of *T. parthenium* as the reducing and stabilizing agent. UV–vis spectra and FT-IR results showed that polyphenols, proteins, polysaccharides, and lipids could be useful for bio-reduction, capping, and stabilizing the particles. The crystalline structure and spherical shape of particles with a size range from 13–25 nm were designated by XRD and FTIR analysis-. CuO-NPs showed suitable catalytic activities in degradation process of the Methylene Blue, Methylene Orange, Rhodamine B, and Congo red by $NaBH_4$. CuO-NPs revealed vigorous antimicrobial and cytotoxic activities against -pathogenic microbial strains (two bacterial and four fungal strains) and A549, Hela, and MCF7 cancer cell lines. This antimicrobial and anticancer activity could be related to the smaller size and the larger surface area of CuO-NPs. Moreover, electrostatic interactions, increased ROS generation, DNA damage and apoptosis induction might be the other effects of CuO-NPs. Our results suggested that CuO-NPs synthesis using aqueous extract of *T. parthenium* can be considered as a suitable candidate for biomedical, pharmaceutical, and environmental applications.

Material And Method

Preparation of T. parthenium **extract**

Fresh leaves and flowers of *T. parthenium* were collected from Kepin, Mazandaran, Iran. The leaves and flowers were washed to eliminate the dust particles. Washed leaves and flowers were then dried and chopped using a mixer. 20g of prepared leaf and flower powder were added to 150 mL warm deionized water and the mixture was maintained in magnetic stirrer for 30 min at 80ºC. The mixture was then centrifuged at 6500 rpm, and the supernatant was filtered by Whatman No.1 filter paper.

Synthesis Of Cuo-nps

In order to prepare CuO-NPs, 35 ml of prepared extract was added to a stirred $CuSO_4$ solution (100 ml, 0.03 M). The mixture was stirred on a magnetic stirrer for 2h at 70ºC and then the caramel brown precipitate was centrifuged at 6500 rpm for 30 min. The resulting precipitate was washed with DI water and then dried at 60˚C in the oven.

Characterization Of Cuo-nps

Different analytical techniques were used to confirm the biosynthesized CuO-NPs. UV-Vis Spectroscopy was used with a different wavelength between 200-650nm for confirming the production CuO-NPs mediated by *T. parthenium* extract. Identification of chemical composition of CuO-NPs was done by FT-IR

Spectroscopy with a wide range of wavenumbers of 400 cm^{-1} to 4000 cm^{-1}. X-ray Diffractometer (XRD) was conducted to identify the crystalline structure of the CuO-NPs in the 2θ domain of 20–80º. The structural characterization of CuO-NPs was determined using FESEM and EDX.

Catalytic Reduction Study Of Dyes

200 µg of CuO-NPs catalyst and 3ml of each dye solution (Congo red and Methylene orange 0.08 mM; Methylene blue 0.03 mM and Rhodamine B 0.05M) were mixed and then 0.5 ml of NaBH4 aqueous solution (6×10^{-3} M) was added to this mixture. The reduction process was monitored using UV-vis spectroscopy and the absorbance was recorded every 25 seconds intervals. The rate constant could be appraised by pseudo-first-order kinetics for dyes reduction. The following equation was applied to determine the rate constant (k_t) of CuO-NPs: $k_t = -\ln (C_t/C_0)$. Where k is the rate constant at the given time and t is the reaction time. C_0 and C_t are the concentrations of dyes at initial and at time t respectively.

The degradation percentage was computed from the formula, $R (\%) = (A_0 - A_t / A_0) \times 100$

Where R (%) is the degradation percentage, A_0 and A_t are the absorbance of a dye at times t = 0 and t = t, respectively. For the recyclability test, the recovered catalyst was washed with distilled water, dried and used in the previous condition.

Antimicrobial Properties Of Cuo-nps

Disc diffiusion method was used to investigate the growth inhibition activity of CuO-NPs against some microbes. The bacterial and fungal strains used for the study were *Escherichia coli, Salmonella typhimurium*, *Fusarium semitectum, Fusarium thapsinum, Candida albicans*, and *Cryptococcus neoformans*. Mueller-Hinton Agar and Sabouraud dextrose agar plates were inoculated with a microbe suspension for bacterial and fungal strains. Various concentrations of CuO-NPs were loaded on sterile paper discs (6 mm in diameter). The bacteria and the fungi plates were incubated at 37°C for 24h and 28°C for 48h, respectively.

Cytotoxic Activity

In vitro inhibitory activities of CuO-NPs obtained by *T. parthenium* extract on MCF7, Hela, A549, and normal fibroblast L29 cells were examined using MTT assay. The cell lines were cultivated on the RPMI-1640 media containing fetal bovine serum 1% (10%), glutamine (1%) Streptomycin and penicillin (100 U/ml) under CO2 5% for 24h at 37°C. The medium was sent out and refilled with fresh medium along with various concentrations of CuO-NPs (25–130 µg/mL) and incubated for 24h at 37°C. Then tetrazolium MTT solution was added to each well and incubated for a further four h. The MTT solution was then

discarded, and the crystals formed were solved by adding DMSO. The optical density of the solutions was read at 570 nm by a microplate reader. The IC50 values and cell viability percentage for each cell line were computed by the following formula.

$$\text{Cell viability}(\%) = \frac{A_{570nm} \text{ of treated cells}}{A_{570nm} \text{ of control cells}} \times 100$$

Declarations

Acknowledgments

This research was financially supported by Amol University of Special Modern Technologies.

References

1. Leszczynski, J., Bionanoscience: nano meets bio at the interface. *Nat. Nanotechnol.***5**, 633–634 (2010).
2. Raigond, P., Raigond, B., Kaundal, B., Singh, B., Joshi, A., & Dutt, S. Effect of zinc nanoparticles on antioxidative system of potato plants. *J. Env. Biol.***38**, 435(2017).
3. Zhang, P., Cui J., Mansooridara, S., Kalantari, A.S., Zangeneh, A., Zangeneh, M.M., Sadeghian, N., Taslimi, P., Bayat, R. & Şen, F. Suppressor capacity of copper nanoparticles biosynthesized using *Crocus sativus* L. leaf aqueous extract on methadone-induced cell death in adrenal phaeochromocytoma (PC12) cell line. *Sci. Rep.***30**, 21236(2020).
4. Sathiyavimal, S. Vasantharaj, S., Bharathi, D., Mythili, S., Manikandan, E., Kumar, S.S., Pugazhendhi, & Pugazhendhi, A., Biogenesis of copper oxide nanoparticles (CuO-NPs) using *Sida acuta* and their incorporation over cotton fabrics to prevent the pathogenicity of Gram negative and Gram positive bacteria. J. Photochem. Biol. **188**, 126–134(2018).
5. Bezza, F.A., Tichapondwa, S.M., & Chirwa, E.M.N. Fabrication of mono dispersed copper oxide nanoparticles with potential application as antimicrobial agents. *Sci. Rep.* **10**-16680(2020).
6. Vasantharaj, S., Sathiyavimal, S., Saravanan, M., Senthilkumar, P., Gnanasekaran, K., Shanmugavel, M., Manikandan, E., & Pugazhendhi, A. Synthesis of ecofriendly copper oxide nanoparticles for fabrication over textile fabrics: characterization of antibacterial activity and dye degradation potential, *J. Photochem. Photobiol. B Biol.***191**, 143–149(2019).
7. Singh, J., Kumar, V., Rawat, K.H., & Kim, M. Biogenic synthesis of copper oxide nanoparticles using plant extract and its prodigious potential for photocatalytic degradation of dyes. *Environ. Res.***177**, 108569(2019).
8. Ali, K., Saquib, Q., Ahmed, B., Siddiqui, M.A., Ahmad, J., Al-Shaeri, M., Al- Khedhairy, A.A., & Musarrat, J. Bio-functionalized CuO nanoparticles induced apoptotic activities in human breast carcinoma

cells and toxicity against *Aspergillus flavus*: an in vitro approach, *Process Biochem.***91**, 387–397(2020).

9. Din, M.I., Arshad, F., Rani, A., Aihetasham, A., Mukhtar, M., & Mehmood, H. Single step green synthesis of stable copper oxide nanoparticles as efficient photo catalyst material. *Biomed Mater.***9**, 41–48(2017).
10. Husseiny, M., El-Aziz, M.A., Badr, Y., & Mahmoud, M. Biosynthesis of gold nanoparticles using *Pseudomonas aeruginosa*. *Spectrochim. Acta Part A.***67**, 1003–1006 (2007).
11. Cittrarasu, V., Kaliannan, D., Dharman, K., Maluventhen, V., Easwaran, M., Liu, W.C., Balasubramanian, B., & Arumugam, M. Green synthesis of selenium nanoparticles mediated from *Ceropegia bulbosa* Roxb extract and its cytotoxicity, antimicrobial, mosquitocidal and photocatalytic activities. *Sci. Rep.***11**, 1032(2021).
12. Mohanpuria, P., Rana, N.K., & Yadav, S.K. Biosynthesis of nanoparticles: technological concepts and future applications. *Nano. Res.***10**, 507–517(2008).
13. Vetchinkina, E., Loshchinina, E., Kupryashina, M., Burov, A., Pylaev, T., Nikitina, & V. Green synthesis of nanoparticles with extracellular andintracellular extracts of basidiomycetes. *Peer J.***6**, 5237(2018).
14. Merzlyak, A., & Lee, S.W. Phage as templates for hybrid materials and mediators for nanomaterial synthesis. *Curr. Opinion. Chem. Bio.***10**, 246–252(2006).
15. Ismail, M.I.M. Green Synthesis and Characterizations of Copper Nanoparticles. *Mater. Chem. Phys.***240**, 122283(2020).
16. Nasrollahzadeh, M., Momeni, S.S., & Sajadi, S.M. Green synthesis of copper nanoparticles using *Plantago asiatica* leaf extract and their application for the cyanation of aldehydes using K4Fe (CN) 6. *J. Colloid Interface Sci.* **506**, 471–477(2017).
17. Juárez-Maldonado, A., Ortega-Ortíz, H., Cadenas-Pliego, G., Valdés-Reyna, J., Pinedo-spinoza, J., López-Palestina, C., & Hernández-Fuentes, A. Foliar Application of Cu Nanoparticles Modified the Content of Bioactive Compounds in *Moringa oleifera* Lam. *Agronomy.* **8**, 67(2018).
18. Brown, A.M., Edwards, C.M., Davey, M.R., Power, J.B., & Lowe, K.C. Pharmacological activity of feverfew (*Tanacetum parthenium* (L.) Schultz-Bip.): assessment by inhibition of human polymorphonuclear leukocyte chemiluminescence in-vitro. *J. Pharm. Pharmacol.***49**, 558-61(1997).
19. Calapai, G., & Delbò, M. Assessment report on *Tanacetum parthenium* (L.) Schulz Bip., herba. *Eur. Med. Agency.***3,** 1–40(2010).
20. Kumari, P., Panda, P.K., Jha, E., Kumari, K., Nisha, K., Mallick, M.A. & Verma, S.K. Mechanistic insight to ROS and apoptosis regulated cytotoxicity inferred by green synthesized CuO nanoparticles from Calotropis gigantea to embryonic zebrafish. *Sci. Rep.* **7**, 16284(2017).
21. Suresh, S., Karthikeyan, S., & Jayamoorthy, K. FTIR and multivariate analysis to study the effect of bulk and nano copper oxide on peanut plant leaves. J. Sci. Adv. Mater. Devices. **1**, 343–350(2016).
22. Ramakrishana, M., Babu, D.R., Gengan, R.M., Chandra, S., & Rao, G.N. Green synthesis of gold nanoparticles using marine algae and evaluation of their catalytic activity. J. Nanostructure. Chem. **6**, 1–13(2015).

23. Abboud, Y., Eddahbi, A., Bouari, A.E., Aitenneite, H., Brouzi, K., Mouslim, J. Microwave-assisted approach for rapid andgreen phytosynthesis of silver nanoparticles using aqueousonion (Allium cepa) extract and their antibacterial activity. J. Nanostructure. Chem. **3**, 84(2013).
24. Arya, A., Gupta, K., Chundawat, T.S. & Vaya, D. Biogenic Synthesis of Copper and Silver Nanoparticles Using Green Alga Botryococcus braunii and Its Antimicrobial Activity. Bioinorg. Chem. Appl. **2018**, 1-9(2018).
25. Sharmila, G., Pradeep, R.S., Sandiya, K., Santhiya, S., Muthukumaran, C., Jeyanthi, J., Kumar, N.M., & Thirumarimurugan, M. Biogenic synthesis of CuO nanoparticle s using *Bauhinia tomentosa* leaves extract: Characterization and its antibacterial application, J. Mol. Struct. **1165**, 288–292 (2018).
26. Pansambal, S., Deshmukh, K., Savale, A., Ghotekar, S., Pardeshi, O., Jain, G., Aher, Y., & Pore, D. Phytosynthesis and biological activities of fluorescent CuO nanoparticles using Acanthospermum hispidum L. extract, J. Nanostruct. **7**, 165–174(2017).
27. Rostami-Vartooni, A. Green synthesis of CuO nanoparticles loaded on the seashell surface using *Rumex crispus* seeds extract and its catalytic applications for reduction of dyes. *IET Nanobiotechnol.***11**, 349–359 (2017).
28. Nagaraj, E., Karuppannan, K., Shanmugam, P., & Venugopal, S. Exploration of Bio-synthesized Copper Oxide Nanoparticles Using Pterolobium hexapetalum Leaf Extract by Photocatalytic Activity and Biological Evaluations. J. Clust. Sci. p. **30**, 1157–1168 (2019).
29. Gowri, M., Latha, N., & Rajan, M. Copper Oxide Nanoparticles Synthesized Using Eupatorium odoratum, Acanthospermum hispidum Leaf Extracts, and Its Antibacterial Effects against Pathogens: a Comparative Study. *BioNanoScience*. **9**, 545–552 (2019).
30. Manjari, G., Saran, S., Arun, T., Rao, A.V., & Devipriya, S.P. Catalyticand recyclability properties of phytogenic copper oxide nanoparticles derived from aglaia elaeagnoidea flower extract, J. Saudi Chem.Soc. **21**, 610-618 (2017).
31. El-Sheikh, S.M., Ismail, A.A., & Al-Sharab, J.F. Catalytic reduction of p-nitrophenol over precious metals/highly ordered mesoporous silica. New J. Chem. **37**, 2399-2407 (2013).
32. Issaabadi, Z., Nasrollahzadeh, M., & Sajadi, S.M. Green synthesis of the copper nanoparticles supported on bentonite and investigation of its catalytic activity. J. Clean. Prod. **142**, 3584–3591 (2017).
33. Ghosh, B.K., Hazra, S., Naik, B., & Ghosh, N.N. Preparation of Cu nanoparticle loaded SBA-15 and their excellent catalytic activity in reduction of variety of dyes. Powder Technol. **269**, 371–378 (2015).
34. Chauhan, A., Verma, R., Kumari, S., Sharma, A., Shandilya, P., Li, X., Batoo, K.M., imran, A., Kulshrestha, S. & Kumar, R. Photocatalytic dye degradation and antimicrobial activities of pure and Ag-doped Zno using cannabis sativa leaf extract. *Sci. Rep.* **10**, 7881(2020).
35. Junejo, Y., Baykal, A., Safdar, M., & Balouch, A. A novel green synthesis and characterization of Ag NPs with its ultra-rapid catalytic reduction of methyl green dye, Appl. Surf. Sci. **290**, 499–503 (2014).
36. Rajeshkumar, S., Menon, S., Kumar, S.V., Tambuwala, M.M., & Bakshi, H.A. Antibacterial and antioxidant potential of biosynthesized copper nanoparticles mediated through *Cissus arnotiana*

plant extract. J. Photochem. Photobiol. B Biol. 197, 111531(2019).

37. Ibrahim, S., Ahmad, Z., Manzoor, M.Z., Mujahid, M., Zahra Faheem, Z. & Adnan, A. Optimization for biogenic microbial synthesis of silver nanoparticles through response surface methodology, characterization, their antimicrobial, antioxidant, and catalytic potential. *Sci. Rep.* **11**,770(2021).
38. Khorrami, S., Zarrabi, A., Khaleghi, M., Danaei, M., & Mozafari, M. Selective cyto-toxicity of green synthesized silver nanoparticles against the MCF-7 tumor cell lineand their enhanced antioxidant and antimicrobial properties. Int. J. Nanomed. **13**, 8013–8024 (2018).
39. Wongrakpanich, A., Mudunkotuwa, I.A., Geary, S.M., Morris, A.S., Mapuskar, K.A., Spitz, D.R., Grassian, V.H., & Salem, A.K. Size-dependent cytotoxicity of copper oxide nanoparticles in lung epithelial cells, Environ. Sci. Nano. **3**, 365–374 (2016).
40. Li, R., Pan, Y., Li, N., Wang, Q., Chen, Y., Phisalaphong, M., &u Chen, H. Antibacterial and cytotoxic activities of a green synthesized silver nanoparticles using corn silk aqueous extract, Colloid Surf. A Phys. Eng.**598**, 124827(2020).
41. Vijayan, R., Joseph, S., & Mathew, B. *Indigofera tinctoria* leaf extract mediated green synthesis of silver and gold nanoparticles and assessment of their anticancer, antimicrobial, antioxidant and catalytic properties. Artif. Cells Nanomed. Biotechnol. **46**, 861–871 (2018).
42. Pugazhendhi, A., Prabhu, R., Muruganantham, K., Shanmu-ganathan, R., & Natarajan, S. Anticancer, antimicrobial andphotocatalytic activities of green synthesized magnesium oxidenanoparticles (MgONPs) using aqueous extract of Sargassum wightii. J. Photochem. Photobiol. B**190**, 86–97 (2019).

Figures

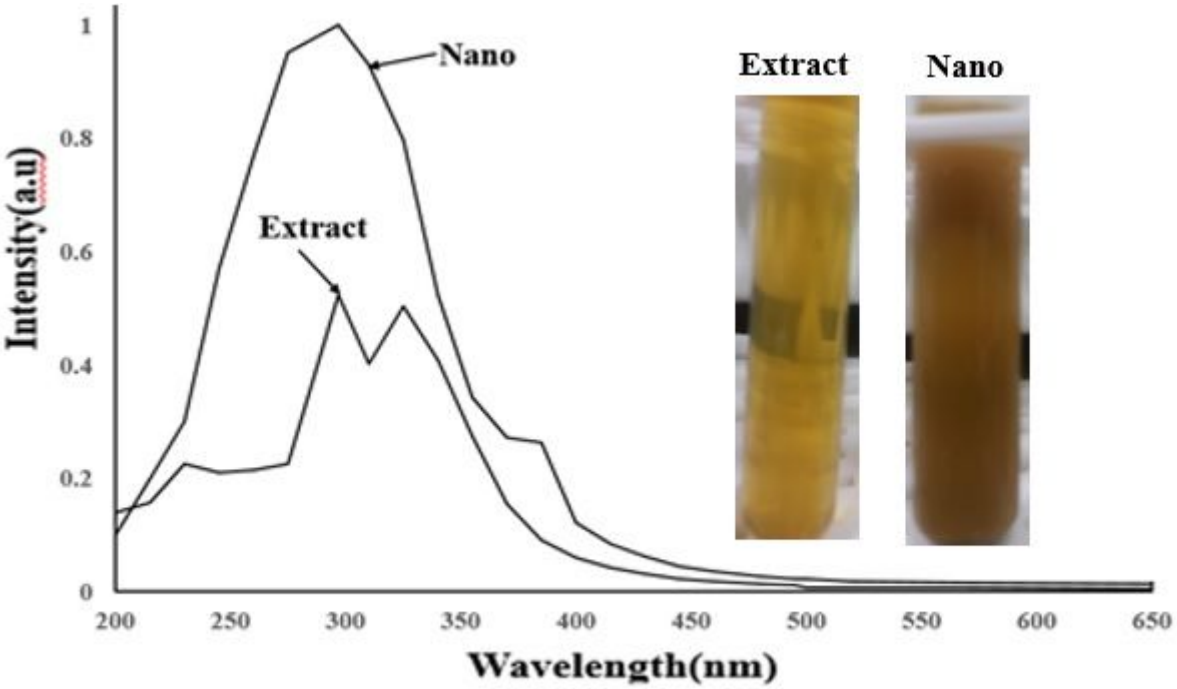

Figure 1

UV-Vis spectra of T. parthenium extract and synthesized CuO-NPs using extract of T. parthenium

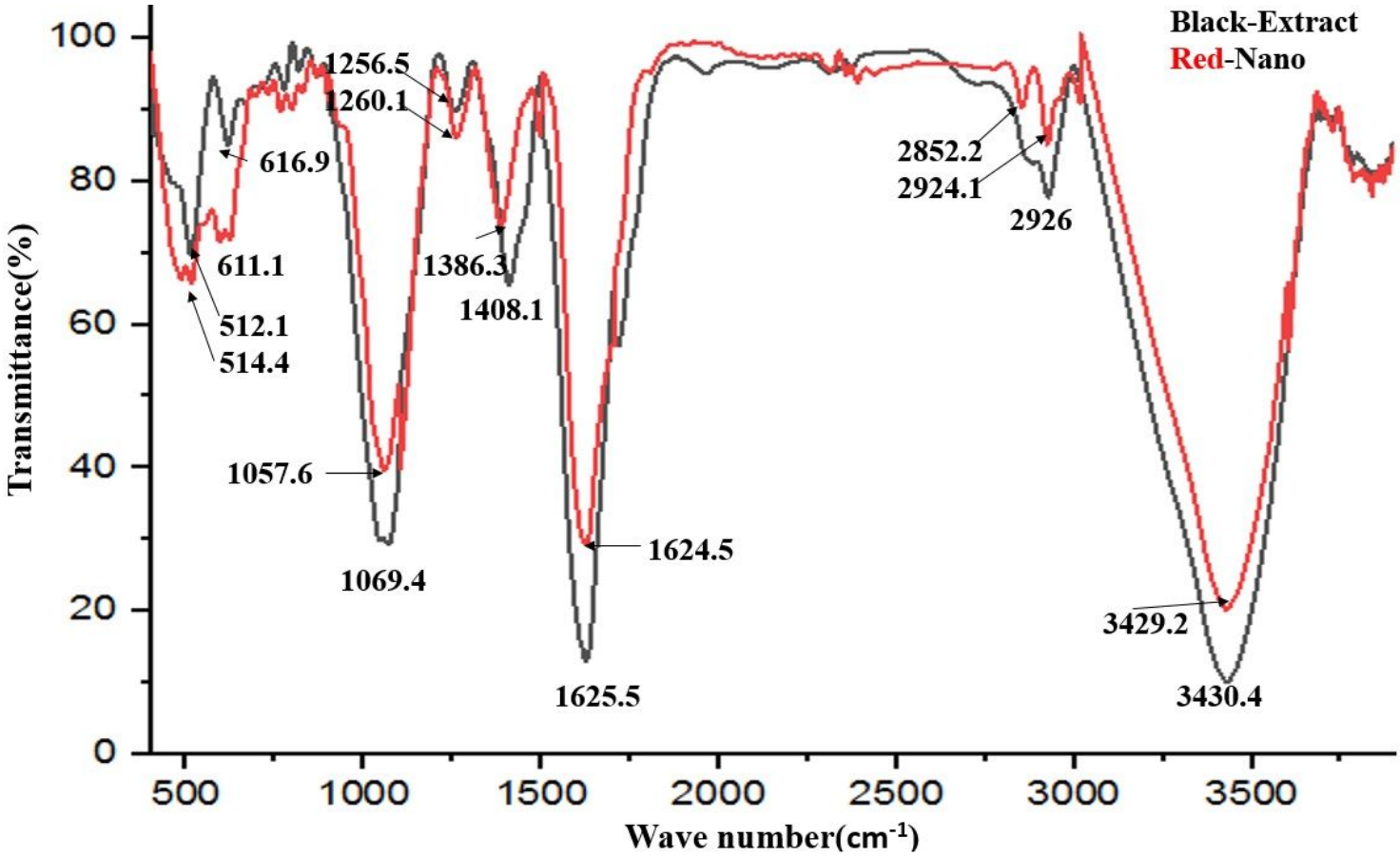

Figure 2

FTIR spectra of T. parthenium extract (Black) and synthesized CuO-NPs by T. parthenium extract (Red)

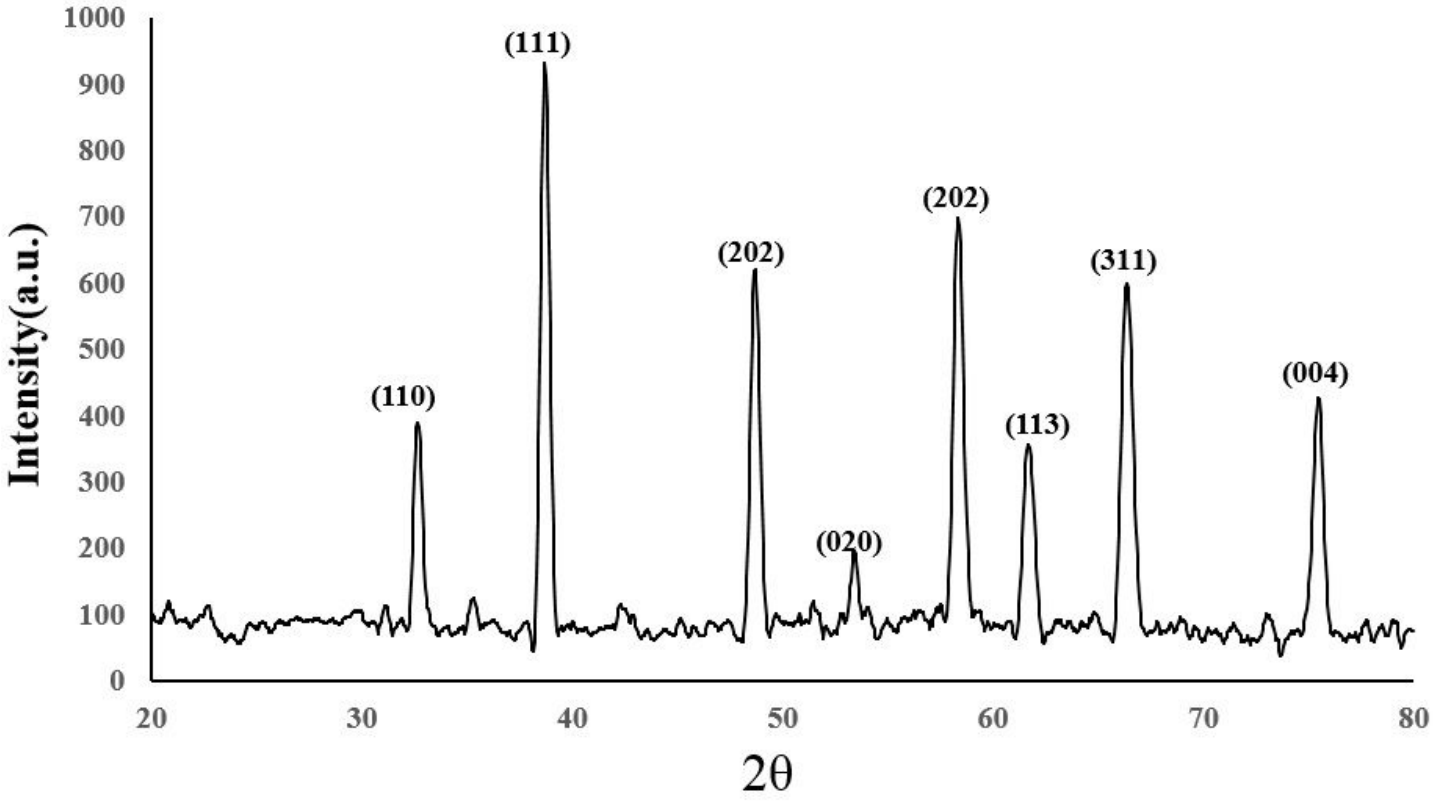

Figure 3

XRD pattern of biosynthesized CuO-NPs by T. parthenium extract

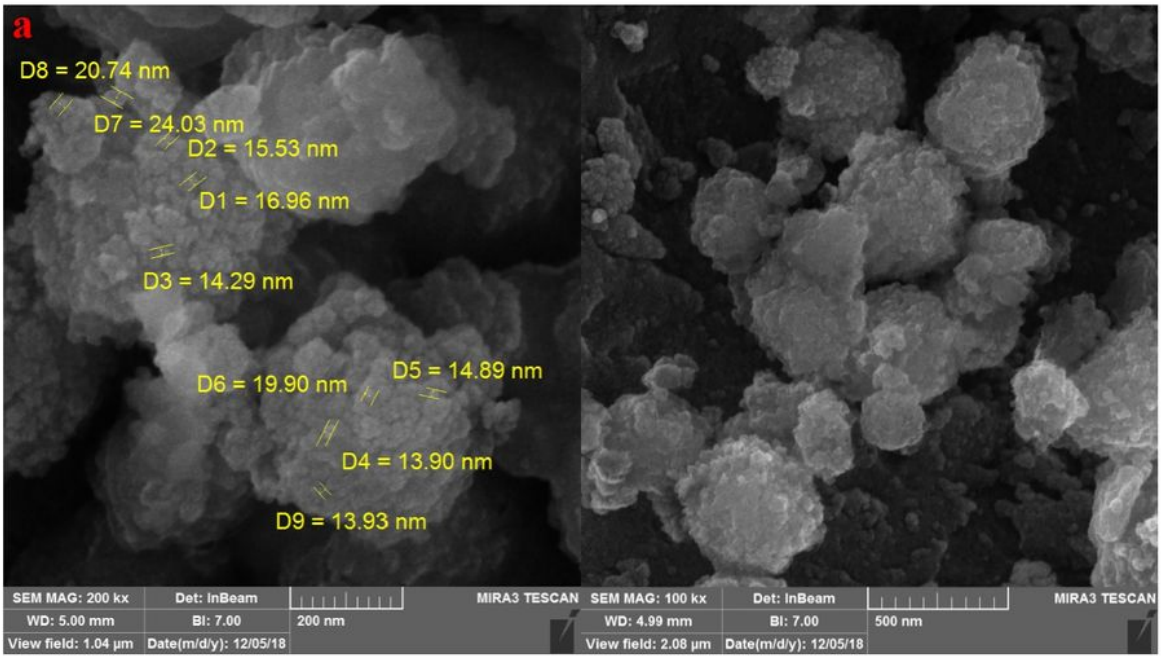

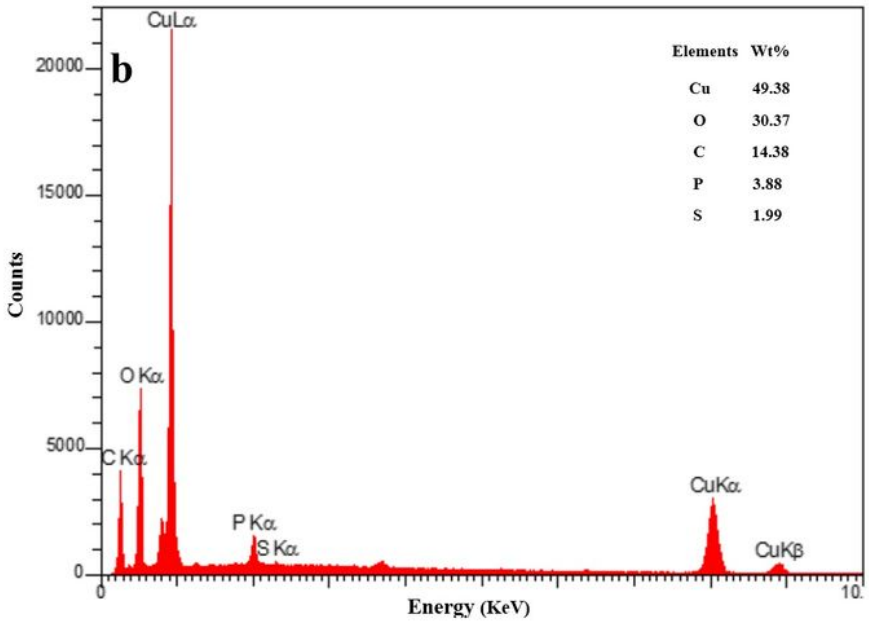

Figure 4

FESEM image (a) and EDX spectra (b) of CuO-NPs synthesized using T. parthenium extract

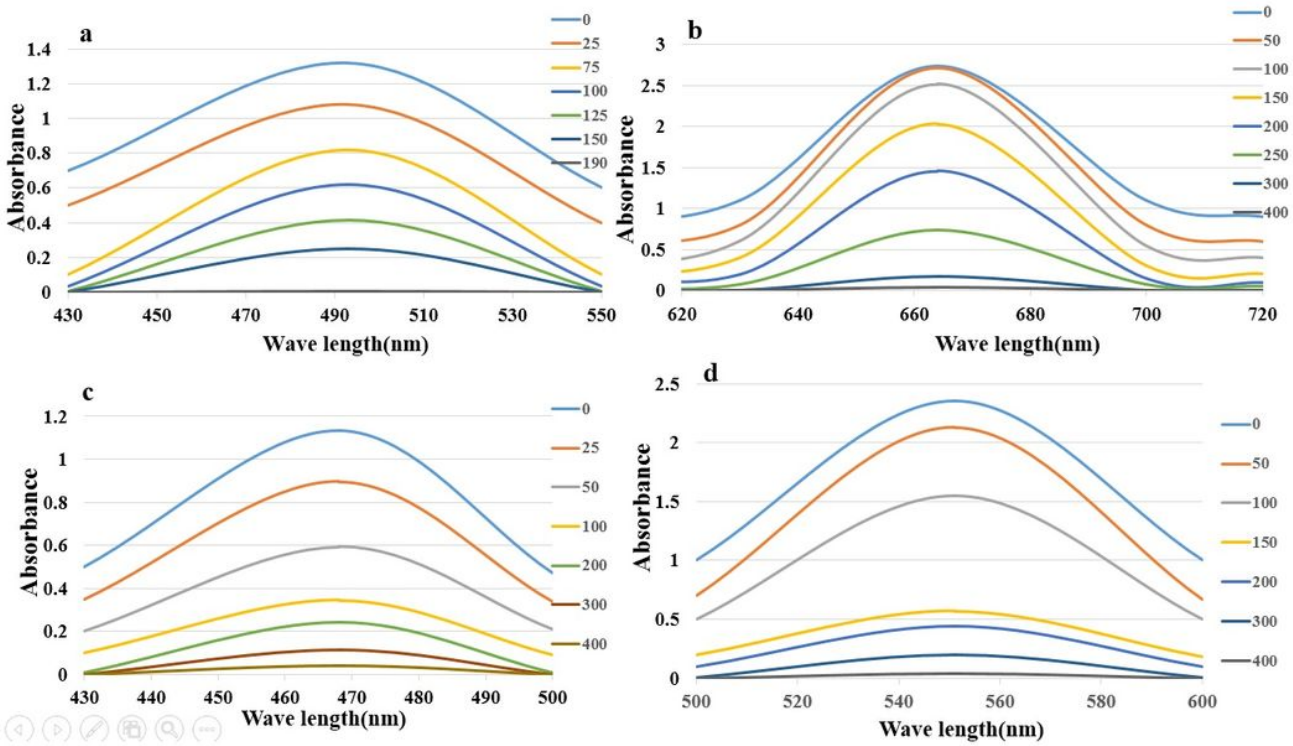

Figure 5

UV–Vis spectra of the reduction of CR(a), MB(b), MO(c) and RhB(d) by CuO-NPs

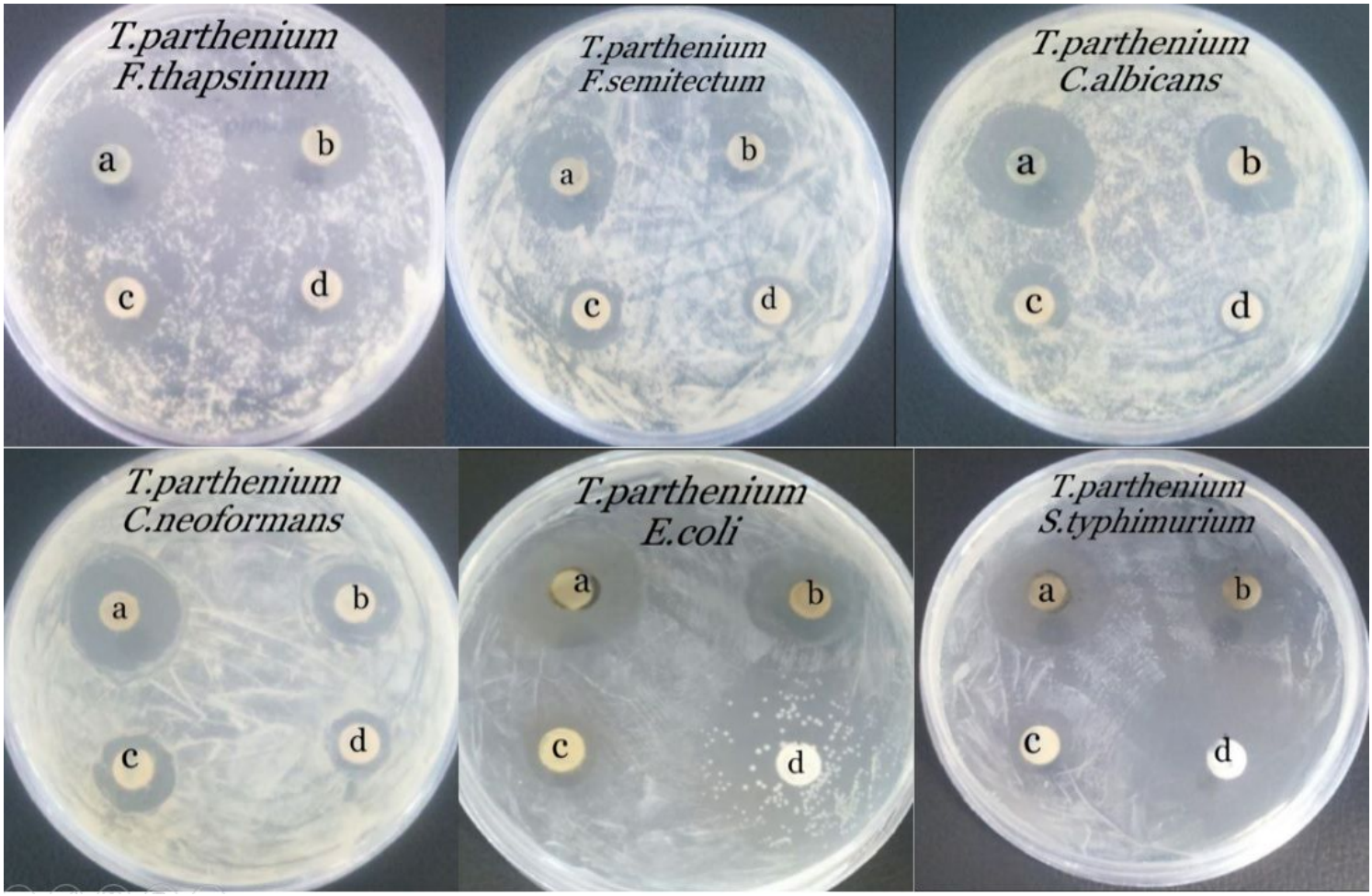

Figure 6

Zone of inhibition of T. parthenium extract derived CuO-NPs against bacteria (a 100 µg/ml, b 70 µg/ml, c 35µg/ml and d Ciprofloxacin) and fungi (a 130 µg/ml, b 100 µg/ml, c 70 µg/ml and d 35µg/ml)

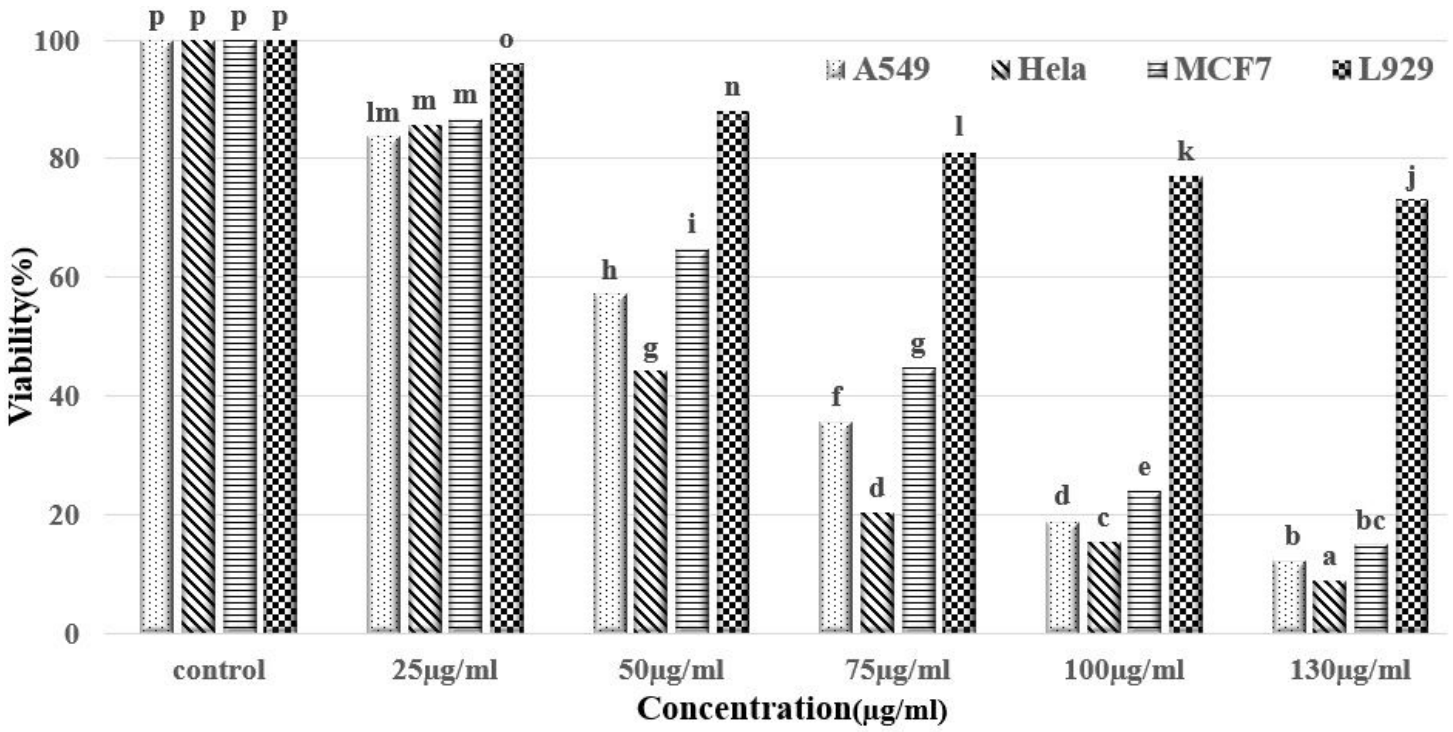

Figure 7

Cytotoxic effects of CuO-NPs against the A549, Hela, MCF7 and L929 at various concentrations (control, 25, 50, 75, 100 and 130 µl/mL)